

# Noise and Gain Characterization of LISA Photoreceivers prior to Irradiation

J. Pulido<sup>1</sup>, P. Colcombet<sup>2</sup>, S. Bruhier<sup>2,3</sup>, Dr. N. Dinu-Jaeger<sup>2,3</sup>

<sup>1</sup> *California State University: Dominguez Hills, Carson, CA, United States, 90745*

<sup>2</sup> *ARTEMIS Lab, Observatoire de la Côte D'Azur, 06300 Nice, France*

<sup>3</sup> *French National Centre for Scientific Research, CNRS, 75016 Paris, France*

(Dated: July 30, 2022)

Photoreceivers are one of the most fundamental components of the Laser Interferometer Space Antenna (LISA) instrument for the detection of gravitational waves. The photoreceivers will be installed on LISA optical benches and they will measure LISA optical heterodyne signals. They must feature low noise to allow a good signal-to-noise ratio. This report presents the important electrical characteristics of the photoreceivers such as noise, gain and bandwidth. The experimental and data analysis methodology is presented. Measurement set-up stability and the reproducibility of the measurements are discussed. This work was performed on different photoreceivers prior to proton irradiation.

## I. INTRODUCTION

The Laser Interferometer Space Antenna (LISA) is a mission currently conducted by the European Space Agency (ESA) in collaboration with National Aeronautics Space Agency (NASA) and with contribution from 16 member states. The LISA mission will be composed of three satellites forming an equilateral triangle formation of 60° degrees and separated by 2.5 million kilometers from each other. Furthermore, the spacecraft will fly along the Earth-like heliocentric orbit and rotate with the solar panels facing the sun to acquire solar energy [1]. LISA will be at 1 AU (150 million km) from the sun and around 50 to 65 million kilometers from Earth for communication purposes. The sun will also make an angle of approximately 20° degrees to the Earth and the configuration of the spacecraft (See Figure 1) [2].

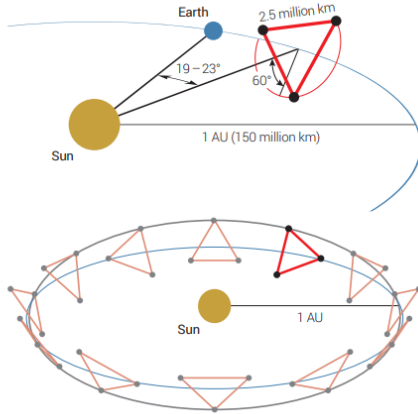


FIG. 1: Graphical Illustration of LISA Orbit. [4]

LISA will be able to detect low-frequency gravitational waves from 0.1Hz to 1Hz while terrestrial gravitational wave detectors like the Laser Interferometer Gravitational-Wave Observatory (LIGO) and VIRGO Observatory can detect high-frequency gravitational waves of 10Hz to 10kHz [2]. This will open the possibility to study small variations caused by gravitational waves and explore new phenomena in the Universe. The phenomena include binary star formation, fundamentals of gravity, merger history of massive black holes, study the rate of expansion in the universe, and much more. Each payload will be made of two Moving Optical Sub-Assembly (MOSA). Each MOSA includes the optical bench, the telescope, the Gravitational Reference Sensor (GRS) along with enclosed test masses, and the MOSA support structure (See Figure 2). The GRS contains a free-falling test mass and the hardware surrounding it to correct all non-gravitational accelerations on the satellites [2].

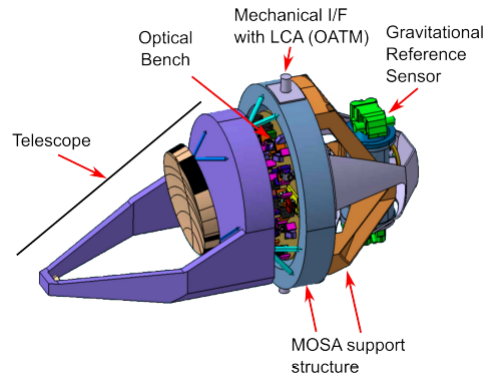


FIG. 2: Images of LISA Moving Optical Sub-Assembly (MOSA). [4]

There are a total of 6 optical benches (OB) in the whole constellation. In each OB, there are three primary interferometers: one reference interferometer, one interspacecraft interferometer, and one test-mass interferometer [2]. A preliminary OB design has been developed by the University of Glasgow and it will contain two faces. The top face (or surface) is often referred as ‘A side’ and the bottom surface is known as ‘B side’ (See Figure 3). In this OB layout, the photoreceivers are displayed on the ‘B side’, which are the components I tested during my internship at ARTEMIS Lab.

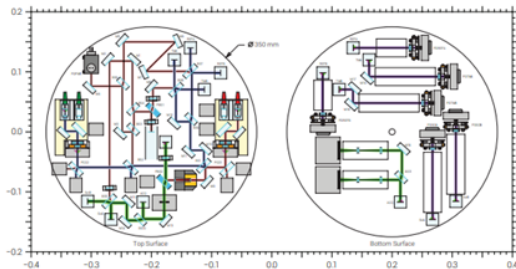


FIG. 3: Possible Layout for the LISA Optical Bench.[4]

### A. ARTEMIS Lab

The Laboratoire d’ Astrophysique Relativiste, Théories, Expériences, Métrologie, Instrumentation, Signaux (ARTEMIS) is a research team located in the Observatoire Côte d’Azur (OCA) in Nice, France. They are also part of the Université Cote d’Azur and the Centre National de Recherche Scientifique (CNRS). This public laboratory is comprised of specialized scientists in the field of signal processing, lasers, mathematics, and astrophysicists interested in the detection of gravitational waves. Additionally, they are involved in research pertaining to Virgo, Einstein Telescope, and LISA. The ARTEMIS group currently makes contributions to LISA instrumentation on data analysis, orbitography, simulations, preparation for LISA satellite assembly, integration and test of the instrument before launch, and photoreceiver radiation studies [3]. Particularly, the clean room historically named MATISSE within ARTEMIS works on the electro-optical characterization of photoreceivers (See Figure 4). This report is focused on three parameters characterizing the photoreceiver, namely noise, gain, and bandwidth. This requires both experimental and computational work that will be described in the following chapters.

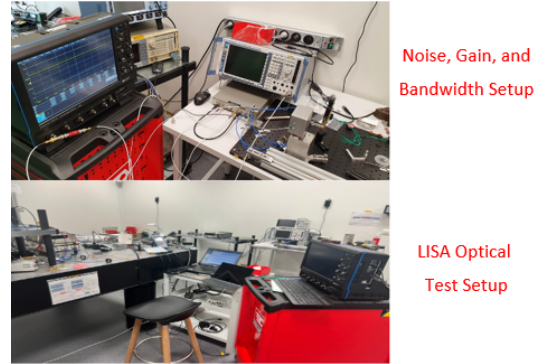


FIG. 4: The Clean Room MATISSE at the Observatoire Côte d’Azur (OCA).

### B. The Photoreceiver

There will be 4 Quadrant Photoreceivers (QPRs) per interferometer and 12 per Optical Bench, which means that there will be a total of 72 QPR for the whole constellation. They will be in the ‘B side’ of the OB [4]. These specific photoreceivers will be part of the Photo Detection System (PDS) and it will have an important role in measuring LISA MHz heterodyne signals for the Phase Measurement Subsystem (PMS) [4]. The optical bench along with the 12 photoreceivers (represented in the grey boxes) can be seen in Figure 5.

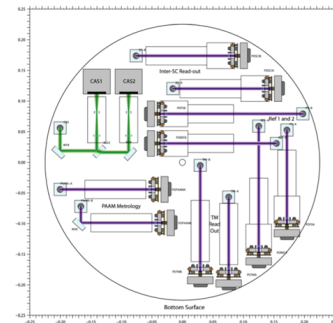


FIG. 5: Representation of the “B-Side” in the OB optical design.[4]

### C. Internship Objectives

The initial goals for this project were to characterize critical Quadrant Photoreceiver (QPR) parameters like noise and gain under Proton Irradiation. This was to observe if there is any degradation on the performance. The irradiation campaign was planned for May 2022; however,

this was not possible due to a measurement instrument that needed to be replaced. The process was postponed until September 2022. My new project is determining the gain and noise of LISA Quadrant Photoreceivers prior to Irradiation. This involves testing Quadrant Photodiodes (QPDs) from different manufacturers. It also entails testing with a variety of FEEs designed and manufactured in Germany. During my internship at ARTEMIS laboratory, in the period from June 1, 2022 to July 30, 2022, I have carried out experimental measurements and I have processed the raw data using Python and MATLAB. I also contributed to the physical interpretation of the results. I am under the guidance of my supervisor Dr. Nicoleta Dinu-Jaeger and I am working closely with my mentors Paul Colcombet and Sara Bruhier.

## II. PHOTORECEIVER DESCRIPTION AND COMPONENTS

Photoreceivers are composed of three main components that allow light to convert into electrical signals and amplify them respectively. In this case, they are a four-channel Quadrant Photodiode (QPD), a Front-End Electronics (FEE), and a faraday cage or a support box (See Figure 6). They also contain power supply cables, a mount support, four female SMA connectors, and other tools to mechanically fix the components.

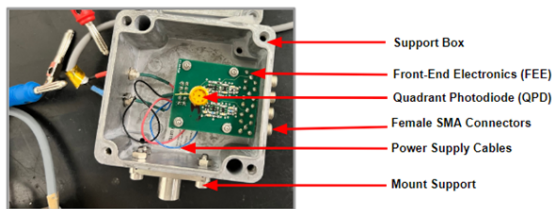


FIG. 6: Schematic of LISA Photoreceivers.

### A. Quadrant Photodiode (QPD)

Photodiodes are the main component of photoreceivers that converts light to electrical signals. It is a photodiode with four segments separated by a small gap and each segment represents an optical-active channel (See Figure 7A). They are manufactured in InGaAs technology since it has good efficiency to the LISA wavelength of 1064 nm and they come in two different package sizes: TO5 and TO8. The package presents six pins where the four short legs correspond to four segment anodes, one long leg corresponds to a common cathode, and the other one is unused (See Figure 7B).

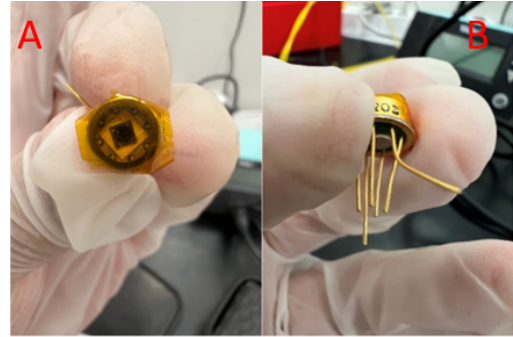


FIG. 7: Pictures of a QPD with 1.5mm diameter.

There is a total of 21 QPDs in the clean room at zone MATISSE. They come from different manufacturers, and they also have different diameters (0.5mm, 1.0mm, 1.5mm, and 2mm). Since QPDs are very sensitive to static electricity, it is important to wear an anti-static wristband to avoid damaging the photodiodes (See Figure 8).



FIG. 8: Anti-Static Wristband for QPD Manipulation.

### B. Front-End Electronics (FEE)

They are a circuit with four transimpedance amplifiers (TIA) that both convert the QPD photocurrent into voltage and amplify the signal. The FEE board has two functional sides, each of them hosting TIAs components of two channels. In addition to this, on one side there are four (or six) pre-soldered sockets to insert the QPD legs (See Figure 9A). On the other side, there are four SMA female connectors for the readout of the four QPR channels, as well as a 10-pin PCI male connector for the QPR

power supply (See Figure 9B). Each side corresponds to two TIAs for two channels (See Figure 9). There are a total of 9 FEEs in zone MATISSE with the same characteristics. 5 FEEs have four pre-soldered sockets to test two QPDs in TO5 package. Conversely, 4 FEEs have six pre-soldered sockets to test one QPD in TO8 package. This is again due to the different package sizes (TO5 and TO8) for each QPD.

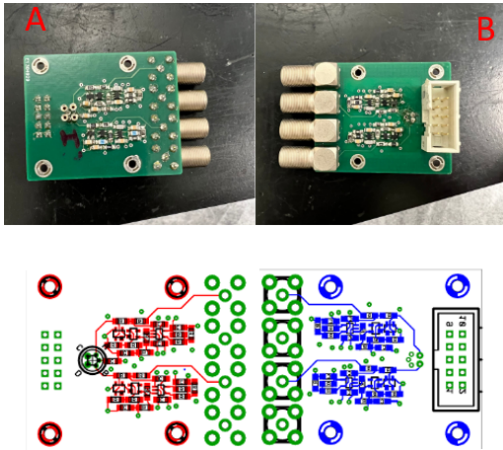


FIG. 9: Picture and Illustration of Front-End Electronics (FEE).[5]

### C. Support Box

This box mainly serves as the support system for the photoreceiver (See Figure 6). It is also used as a faraday cage to protect the QPD and the FEE from any electromagnetic fields that could influence the results. Furthermore, it contains a hole in the front to allow the access of light into the QPD and the power supply cables to provide voltage to the photoreceiver (See Figure 10A).

### D. Assembly

I have worked on the assembly of any photoreceiver before measurement in the following way:

1. The FEE has four support legs that aim to stabilize the card inside the support box. I inserted the legs on the wholes on each edge of the FEE (See Figure 9). I also secured the legs using the four individual nuts on the other side until it looks as shown in Figure 9A.
2. I connected the FEE 10-pin PCI male connector to the box power supply connector shown in Figure

10A. I fitted the FEE card inside the box and inserted the 4 SMA female connectors into the box holes. It was necessary to check that the power supply is either off or not connected to the box.

3. I wore the anti-static wristband as shown in Figure 8 and inserted the QPD pins into the FEE pre-soldered sockets accordingly. It is recommended to use a multimeter to test the electrical continuity and make sure it is connected as shown in Figure 5.
4. I closed the support box by screwing the lid onto the box and making sure the box hole is aligned with the position of the QPD. Then, I mounted the photoreceiver on QPR Noise Characterization Setup as shown in Figure 10B. I also secured lightly the mount support of the box to the stand.
5. I connected the red and blue cables (+5V and -5V) into the power supply and turned on the device when ready to start the experiment.



FIG. 10: Photoreceiver Assembly and Mount.

## III. EXPERIMENTAL SETUP

### A. Objective

The setup aims to characterize the noise, gain, and bandwidth of photoreceivers to deduce if the proton irradiation induces any degradation of performances. Moreover, QPDs of different diameters and packages will be tested. The results should feature an input-referred current noise below  $2pA \cdot Hz^{-1/2}$ , in LISA heterodyne range between 5MHz to 25MHz to avoid signal-to-noise ratio degradation [5]. This research is crucial to guarantee the performances of the QPDs during full lifetime of the LISA mission.

### B. Experimental Setup

The setup contains several instruments to measure the voltage noise of photoreceivers. For this purpose, each

photoreceiver output channel is connected successively, through a coaxial cable, to a RS Spectrum Analyzer. This allows to readout the AC voltage signal. In addition, using a T adaptor, a LeCroy oscilloscope is connected in the chain to measure the photoreceiver DC voltage signal. Before sending the AC voltage signal to the RS Spectrum Analyzer, a DC block is used to remove the DC component of the readout signal and to protect the RS instrument. Lastly, an amplifier has been added with the purpose to amplify the Photoreceiver voltage signal over the background instrumental noise. The photoreceiver will be measured in dark and light conditions. For this, a white light source is used in front of the photoreceivers allowing to illuminate the QPD during measurements. (See Figure 11).

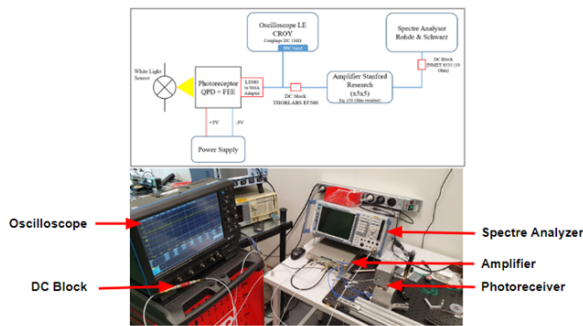


FIG. 11: Noise, Bandwidth, and Gain Setup.

#### IV. METHODOLOGY

The methodology consists of two main steps. Firstly, it entails performing three types of measurements: Instrument Background Noise, Photoreceiver Voltage Noise in dark and in light conditions. Secondly, it is to calculate the input-current noise and gain using Python. During my internship, I participated to all these steps, and I will describe them in the following sections.

##### A. Instrument Background Noise

This measurement is the instrument background voltage noise  $v_{Instrument}$ . Instead of connecting the photoreceiver directly to the oscilloscope, I placed a 50 Block on this end (See Figure 12) to only measure the floor. I made sure the Amplifier is turned on. Furthermore, I set the default standard parameters by loading the file "`CONFIG_LISA.FSP`".

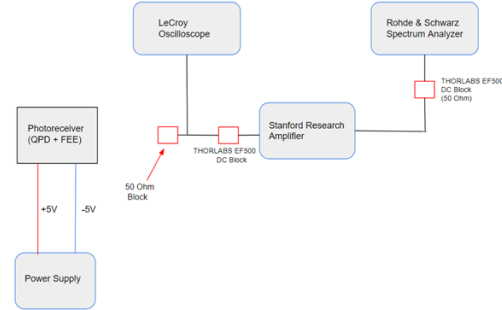


FIG. 12: Setup for Floor Measurement.

##### B. Dark Voltage Noise

This measurement is the dark voltage noise density spectra  $v_{darkmeas}$ . I connected the photoreceiver to the oscilloscope using the adapter (See figure 13). I turned off the white light source and I did a total of four measurements for all four different channels. The DC output voltage must be around 700mV so I wrote down the value given from the oscilloscope since I need it to process the data on python. The **Sweep Count** and **Sweep Time** Parameters must be the same as the Floor Measurement. I measured the output voltage for each QPD channel. To save this file, I followed the same rule as the Floor Measurement but including the segment letter being measured (Channel A, B, C or D).

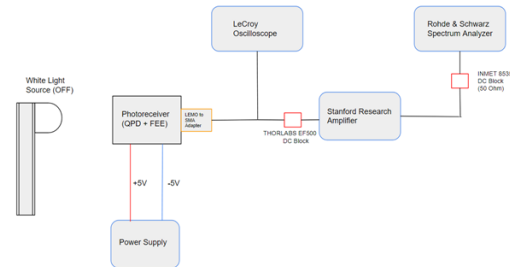


FIG. 13: Setup for Dark Measurement.

##### C. Light Voltage Noise

This is the voltage noise light density spectra  $v_{lightmeas}$ . I kept the same connection as section 4.3. This time I turned the white light source on, and I did the same four measurements for all four channels. (See Figure 14). I adjusted the light source accordingly to shine the desired segment. The DC output voltage should

be close to 0V, however, any value within the range of -200mV to 200mV is acceptable. I also wrote down the output value of each QPD channel to process the data on python. The file was saved as shown in the previous measurements.

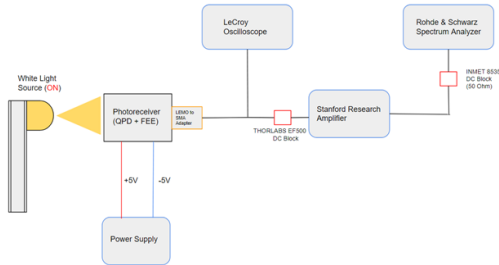


FIG. 14: Setup for Light Measurement.

#### D. Calculating Input-Current Noise and Gain using Python

The voltage noise density spectra in the dark  $v_{dark}$  and light  $v_{light}$  are corrected by subtracting the instrumental noise as indicated in Equation 1 and 2. A Python routine is used for these calculations.

$$v_{dark} = \sqrt{v_{darkmeas}^2 - v_{instrument}^2} \quad (1)$$

$$v_{light} = \sqrt{v_{lightmeas}^2 - v_{dark}^2} \quad (2)$$

After instrumental noise subtraction, the input-current noise  $i_{noise}$  is calculated using Equation 3 where  $i_{shot} = \sqrt{2 \cdot q \cdot I_{DC}}$  is the current noise of the White Light Source and  $q = 1.6 \times 10^{-19} C$  is the elementary electric charge and  $R = 42.2k\Omega$  is the impedance system. The output voltage  $V_{DC}$  is calculated by subtracting the output voltage recorded in Section 4.2 from the output voltage in section 4.3 for each channel.

$$i_{noise} = \frac{v_{dark}}{v_{light}} i_{shot} \quad (3)$$

Moreover, the Transimpedance Gain  $G_{TIA}$  is the gain from the FEE card that amplifies the QPD signal. It can be calculated with the voltage noise density spectra  $v_{dark}$  and  $i_{shot}$  (See Equation 4).

$$G_{TIA} = \frac{v_{dark}}{i_{shot}} \quad (4)$$

The Python program reads the files from each measurement discussed in the methodology section. The code

contains all the equations presented here and it calculates the input-current noise and gain. Furthermore, the script allows the user to input the output voltage  $V_{DC}$ . The Python program also generates a “.csv” file with all the noise and gain values for each QPD channel under the dark or light conditions. This is helpful in case we want to compare the results between QPDs or FEEs.

## V. EXPERIMENTAL RESULTS

I did a total of 43 measurements using the setup. I tested QPDs from three different manufacturers. I used all “.csv.” files generated by the Python code, and I rearranged them on Excel to be able to compare them based on QPD characteristics. I also wrote a code on MATLAB to visualize the data and display the results on this report.

### A. Stability and Repeatability

The first purpose of my work was to check if the noise measurements are stable and reproducible over time. For this, I have examined two photoreceivers, with QPDs of two different diameters, over 4 days. The first QPD has a diameter of 2mm (QPD2001) while the second one is a QPD has a diameter of 1mm (QPD0362). Both QPDs were tested from June 14, 2022, to June 17, 2022. The FEE cards along with their QPDs were mounted and dismantled from the support box after each daily measurement. I took the mean of the noise and gain on one channel over four days. The error was measured by using the Excel command “stdev.s”. The error percentage ranged between 2-10%. I will only provide the results for Channel A and B; however, the results for Channel C and D were very similar. I also showed the range of LISA heterodyne signal (the red dashed lines) to help visualize whether the noise is below  $2pA \cdot Hz^{-1/2}$ .

The dashed blue line named “Threshold” is the limit to feature a good signal-to-noise ratio of  $2pA \cdot Hz^{-1/2}$  at 25 MHz [5] (See Figure 15a and 15b) The noise for Channel A and B were very stable within the LISA heterodyne signal (5MHz to 25MHz). It is worth noting that the noise in both Channel A and Channel B goes beyond the “threshold” line at around 18MHz, which means it could degrade the signal-to-noise ratio. The dashed blue line named ‘Theoretical’ is the gain of the FEE ( $42.2k\Omega$ ). The gain in Channel B shows more stability (See Figure 15d) than the gain in channel A (See Figure 15c) but the curve is very similar.

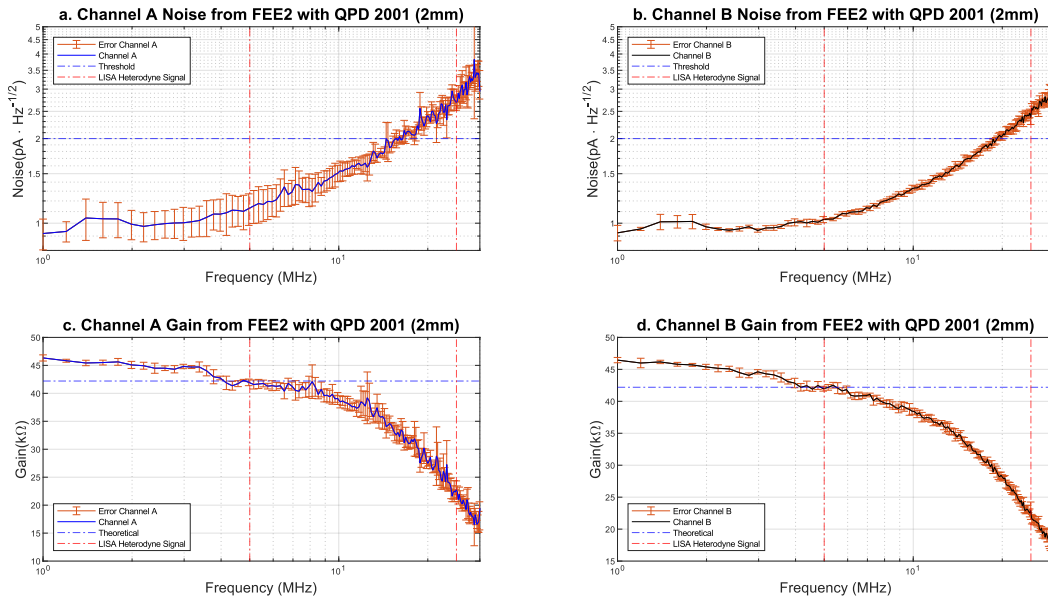


FIG. 15: Stability and Repeatability results of 2mm diameter QPD (QPD2001) for Channel A and B. The top shows the Noise. The bottom shows the Transimpedance Gain of FEE.

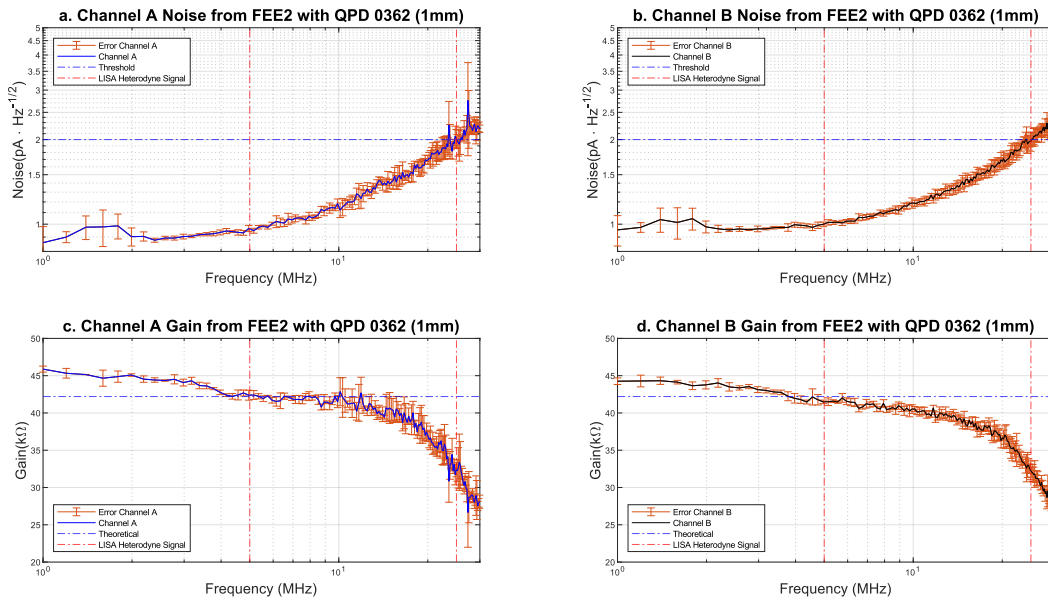


FIG. 16: Stability and Repeatability results for 1mm diameter QPD (QPD0362). The top shows the Noise. The bottom shows the Transimpedance Gain of FEE.

The 1mm QPD also features stability on the noise. The curve appears to be below the  $2 \text{ pA Hz}^{-1/2}$  limit at 25MHz and the errors are very low within the LISA heterodyne signal (See figure 16a and 16b). The 1mm QPD is smaller in diameter than the 2mm QPD, so this might be a reason why the 1mm QPD has lower noise (More details in Section 5.2 and 5.3). The gain in Channel B features more stability (See Figure 16c) than in Channel A (See Figure 16d). The results are often very similar between channels so it is not necessary to show Channel C or D. The errors from those two channels also remain consistent between 2-10MHz. There is a slight bump that appears around 2MHz in the noise measurements for all QPDs; however, this was already a problem with the setup, and it comes from the background noise in the building. This bump also depends on how the photoreceiver is mounted.

### B. 1mm, 1.5mm and 2mm QPD Diameter Results

The project also consisted of characterizing the noise and gain for card FEE2 using three types of QPDs with different diameters. I will only show Channel A results of all 8 photodiodes; however, the results of the other channels are very similar. The first three QPDs of 1mm diameter (QPD 1001, 1002, and 1003) were measured with the parameters of 840 **Sweep Time** and 20 **Average Sweep Count** which are the default LISA measurement parameters for this setup. The remaining QPDs of 1.5mm and 2mm diameter were measured with the pa-

rameters of 110ms **Sweep Time** and 50 **Average Sweep Count** because this improves the signal. (See Figure 17). The QPD diameter influences the measurement results. The smaller diameter QPDs (1mm and 1.5mm) are below the input-current noise threshold while the big QPD (2mm) are beyond the threshold within the range of the LISA heterodyne signal (See Figure 17a). Moreover, the frequency dependence of the gain shows differences in the results for all diameters. The 1mm QPDs have the highest bandwidth than the remaining two sizes (1.5mm and 2mm) (See Figure 17b) The results conclude that smaller QPD diameters feature less noise. Similarly, smaller QPD diameters feature a wider bandwidth. Since smaller diameter means smaller capacitance the capacitance of the QPD is influencing the current.

### C. 0.5mm and 1mm QPDs Diameter Result

FEE2 was also tested two QPDs of 0.5mm and 1mm diameter from another manufacturer. I will also show the results for Channel A of all six photodiodes because the results of the other channels are the relatively the same. They were all measured with the same Spectrum Analyzer parameters of 110ms **Sweep Time** and 50 **Average Sweep Count**. The same principle holds that QPDs with smaller diameters have less noise due to small capacitance (See Figure 18a). Similarly, QPDs with smaller diameters will feature a wider bandwidth (See Figure 18b).

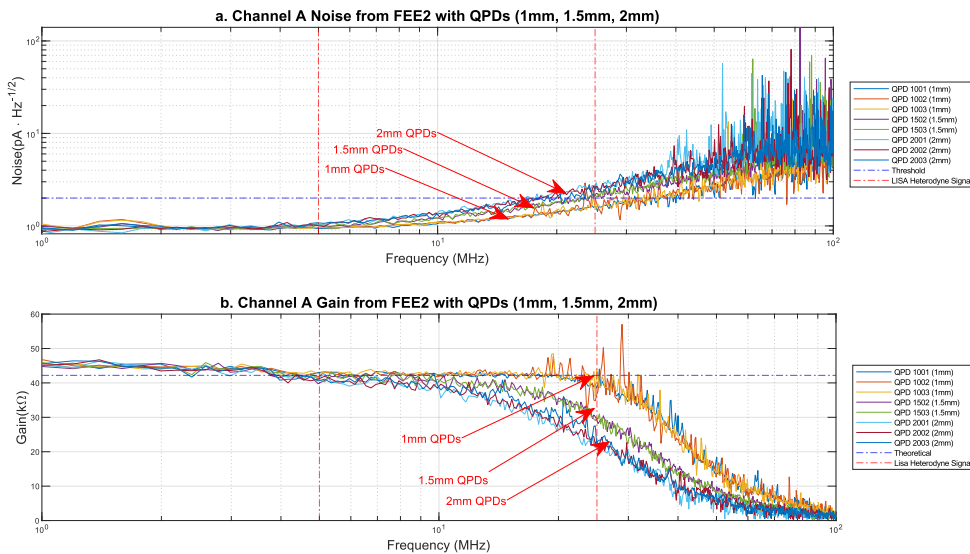


FIG. 17: Three (1mm, 1.5mm, and 2mm) diameter QPD results for Noise, Bandwidth, and Gain.



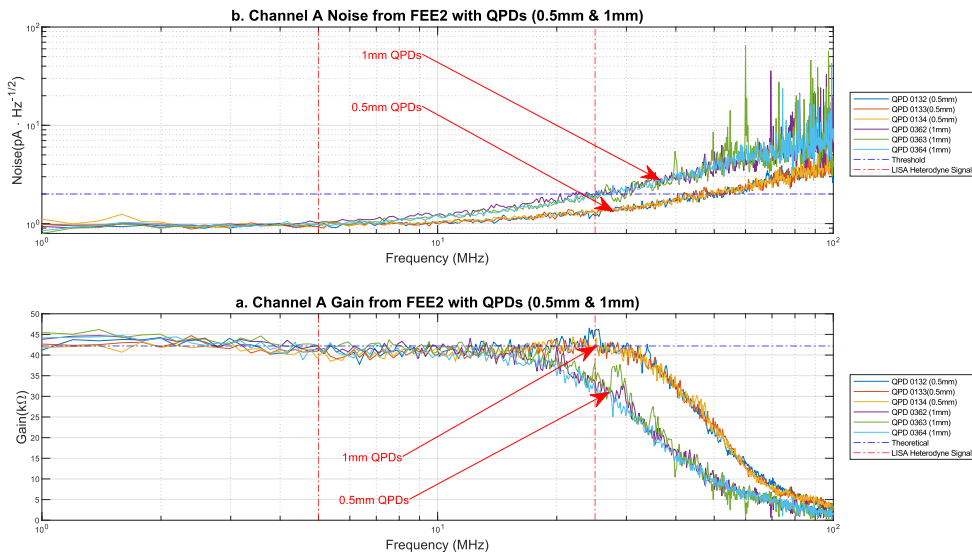


FIG. 18: Noise, Bandwidth, and Gain result from two (0.5mm and 1mm) diameter QPDs.

## VI. PROTON IRRADIATION FACILITY

My project was originally to characterize the electro-optical capabilities of the photoreceivers under proton irradiation. The irradiation period was supposed to occur on May 2022 at the Center Antoine Lacassagne (CAL) in Nice, France. Unfortunately, due to a technical problem with the measurement instrument, the process was postponed until September 2022. I will not be here when the irradiation is done; however, I was able to visit the facility on June 29, 2022.



FIG. 19: The Cyclotron at the Center Antoine Lacassagne (CAL) in Nice, France.

The site has one of the first cyclotrons built in France and it is currently treating children with eye tumor. The

R&D beam line of the 65MeV cyclotron was constructed recently (See Figure 19A) and it will be used for the irradiation test of the photoreceivers. The photoreceivers will be installed at the end of the R&D line on the section presented in Figure 19B. Once the irradiation period is done, the same electro-optical characterization will be performed on the photoreceivers to observe if there is any degradation.

## VII. CONCLUSION

The noise and gain of the photoreceivers are crucial to LISA overall functionality. For this reason, these parameters need to be tested before and after irradiation. The purpose of this internship was to perform voltage noise tests and to calculate the input-current noise and gain for different photoreceivers prior to irradiation. Firstly, we have performed repeatability and stability measurements of the two photoreceivers, featuring two QPD diameters of 1mm and 2mm. They were stable throughout the week featuring less than 10% standard deviation errors within the LISA heterodyne range frequency (5MHz to 25MHz). The comparison between QPD diameters revealed that a higher bandwidth is a result of smaller diameters. Similarly, smaller diameters produce lower noise as shown in section 5.2 and 5.3. The ongoing work for this project is to test the electro-optical characteristics of the pho-

photoreceiver after irradiation. In September, the components will be irradiated, and the same measurements will be done to compare if there are any degradations. This project allowed me to examine the electrical characteristics, as noise and gain, of the photoreceivers for interferometric type measurements like the LISA mission. During the pandemic, I was not able to receive proper manual experimentation with electronics. This internship provided me the tools necessary to not only understand the working principles of photoreceivers, but it also helped me to do manual work like assembling the photoreceivers for noise and gain calculations, soldering FEE cards, and utilize each instrument in the setup. I feel that this REU was also beneficial on the sense that I did data analysis, and I also was able to use my skills on programming languages. Finally, this internship also redefined my passion in research and my desire to continue working on my dream of attending graduate school.

### VIII. ACKNOWLEDGMENTS

I would like to thank Dr. Nicoleta Dinu-Jaeger for her immense assistance with this report, my first hands-on

internship and my overall experience in France. This has been a truly beneficial opportunity that prepared me to do interactive experiments and let me to continue working with programming languages skills such as Python and Matlab or computer software such as Excel. I would also like to thank Paul Colcombet for his extensive work in the setup, for helping me with the python code, and for supervising the experiments. I also want to thank Sara Bruhier for the help with the setup, for supervising my work, and for all the useful explanations as well as documents or figures. I want to thank the ARTEMIS Lab and the QPR Working Group (QPRWG) within the LISA consortium for trusting me with the photoreceivers and allowing me to contribute to their research on LISA QPR flight models. Lastly, I want to thank the National Science Foundation (NSF), Dr. Paul Fulda, and Dr. Peter Wass for providing us with this program and for organizing every single detail in this internship. This project was funded by NSF grants NSF PHY-1950830 and PHY-1460803 through the International REU program by the University of Florida.

- 
- [1] European Space Agency. (2021). Mission Summary. LISA. Retrieved from <https://sci.esa.int/web/lisa/-/61367-mission-summary>
  - [2] Danzmann, K. (2017). "LISA: Laser Interferometer Space Antenna". LISA Consortium. Retrieved from [https://www.elisascience.org/files/publications/LISA\\_L3\\_20170120.pdf](https://www.elisascience.org/files/publications/LISA_L3_20170120.pdf)
  - [3] OCA. (n.d.). ARTEMIS. Retrieved from <https://artemis.oca.eu/fr/rechercheartemis>
  - [4] LISA Instrument Group (2017). LISA Payload Description Document. ESA.
  - [5] Barranco, G. F., Heinzl, G. (2021). A DC-Coupled, HBT-Based Transimpedance Amplifier for the LISA Quadrant Photoreceivers. IEEE Transactions on Aerospace and Electronic Systems, <https://doi.org/10.1109/TAES.2021.3068437>